COMMUNICATION

Light- and Touch-Point Localization using Flexible Large Area Organic Photodiodes and Elastomer Waveguides

By *Robert Koeppe,* Petr Bartu, Siegfried Bauer,* and *N. Serdar Sariciftci*

After the development of efficient organic photodiodes,[1–3] photovoltaic devices are close to being commercialized. However, introducing organic photodiodes to the sensor market shows much less progress. Organic photodiodes can be easily produced in large areas on flexible substrates and lucrative applications for such sensors will have to be found.

Matrices of organic photodiodes combine high sensitivity and spatial resolution with large area production,[4] but covering areas of several square meters with sub-centimetre resolution requires an enormous number of individual diodes with a correspondingly complicated network of conducting interconnects. The cost and complexity of such devices would be similar to large size organic light-emitting television screens, which are currently not available on the market because of high production costs and insufficient reliability.

Simple applications may include large area human interface devices for controlling computers, and machines that could utilize large area photodetectors for tracing a light spot across the surface of, for example, a large projection screen without the need for matrices of sensor elements. While position sensitive detectors (PSDs) using the lateral photoeffect are envisioned using inorganic[5] as well as organic[6] semiconductors, their size is usually limited by the low conductivities of the semiconductors. Another approach to such devices is to use an organic photodiode with a good conducting and a resistive electrode. In such devices, current signals drop across the resistive electrode and depend on the distance between excitation and connection to the outer circuit. This has been realized as one-dimensional strip photodetectors[7] and two-dimensional piezoelectric touchpads based on polymer ferroelectrets.[8]

The devices presented in the following paper utilize a method that allows direct and facile two-dimensional visible lightpoint position detection in a large-area, flexible, and semitransparent device. By adding a silicone elastomer waveguide and light-emitting diodes (LEDs), the device is upgraded to a flexible, large area touchpad that still remains semitransparent and sensitive to the position of an impinging lightspot. Possible applications are interactive screens for presentations and games or artificial skin[9] for robots.

[*] Dr. R. Koeppe, P. Bartu, Prof. S. Bauer
Department for Soft Matter Physics (SoMaP)
JKU Linz, 4040 Linz (Austria)
E-mail: robert.koeppe@jku.at
Dr. R. Koeppe, Prof. N. S. Sariciftci
Linz Institute for Organic Solar Cells (LIOS)
JKU Linz, 4040 Linz (Austria)

DOI: 10.1002/adma.200900557

The PSD is described schematically in Figure 1. The photograph in Figure 1a shows a semitransparent device with an active area of 49 cm^2. The transmission is greenish with a maximum of 37% at 540 nm, which allows mounting of the device in front of a display. In Figure 1a, a sheet of paper that displays the chemical structures of the organic semiconductors is used.

Figure 1b shows a cross section of the device. The same photodiode structure has already been presented as an organic solar cell with high quantum efficiencies over the visible spectrum.[10] The diode is formed between a bottom contact of poly(ethylene dioxythiophenes):poly(styrene sulfonate) (PEDOT:PSS) and an Al top electrode with a 50 nm thin layer of zinc–phthalocyanine (ZnPc) mixed with C_{60} (1: 1 by volume blend) followed by a pure C_{60} thin film of 30 nm.

In contrast to the use as a solar cell, where a high conductivity of the electrodes is essential for efficient power conversion, the electrodes have to be resistive, preferably with a homogeneous sheet resistance. This is achieved by using a poly(ethylene teraphthalate) (PET)-foil substrate precoated with a lower electrode of PEDOT:PSS (Orgacon F-350 and F-1500 with 350 Ω □ and 1.5 kΩ □, respectively). The upper electrode is an evaporated layer of Al with a thickness of ~8.5 nm showing a sheet resistance of 100–200 Ω □. To obtain optimal signal pick-up, Ag and Al metal stripes with 100 nm thickness are deposited along the edges of the electrodes as shown in Figure 1a. The devices are hot-laminated between 150 μm thick PET lamination foils and stored and measured under ambient conditions.

In order to assess the performance of the device, it is placed on top of an *x*,*y*-positioning stage that moves under a laser diode (532 nm, 0.8 mW, chopped at 271 Hz), so that the light spot scans over the surface as indicated in Figure 1a. The signal readout is carried out as shown in Figure 1c. All pickup stripes at the edges of the electrodes are connected by a relay switch to a single lock-in amplifier. For each position of the light spot on the sample, four current signals are measured. The first signal I_1 is measured when channel 1 is connected to the polymer electrode, while channels 3 and 4 are connected to the Al electrode. Signal I_3 is channel 3 connected to the Al and channels 1 and 2 connected to the polymer electrode and so on. The photocurrent signal magnitudes in the present device range between 18 and 78 μA.

These signals are not directly correlated to the position of the light spot. Inhomogenities in the charge generation efficiency and the changing resistance in the opposite channel have a large influence on the current signals. A logarithmic dependence on the position in the *x*- and *y*-direction can be gained as shown in Figure 1d by dividing the current signals. A signal ratio of log (I_a/I_b) can be extracted, where log (I_1/I_2) is directly proportional to the

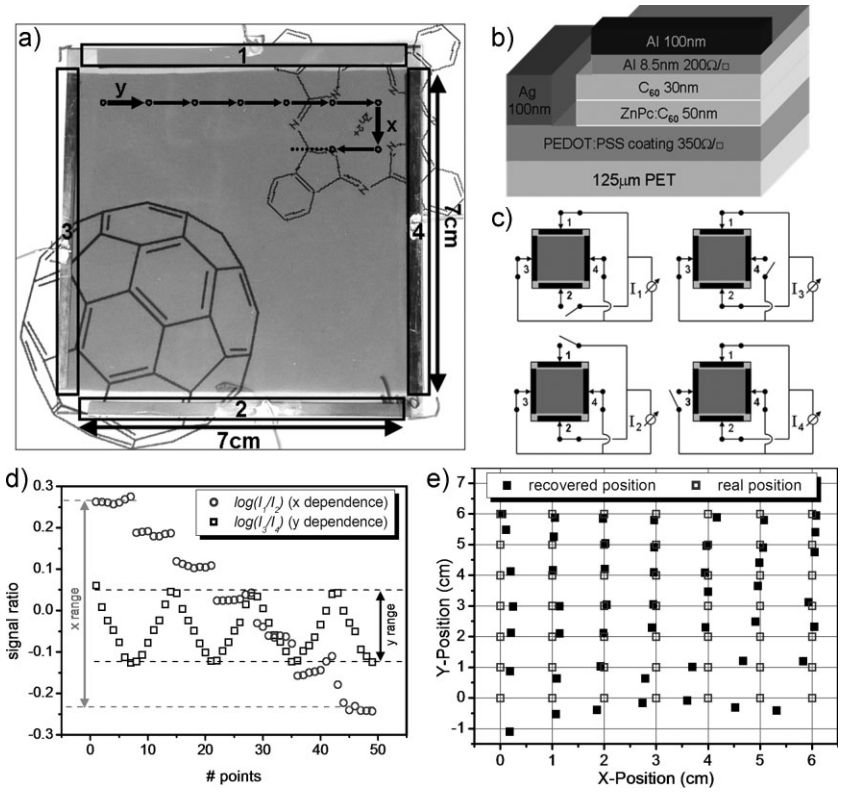

Figure 1. Characteristics of the position sensitive device. a) Top view photograph of the large area photodiode on a sheet of paper with the chemical structures of the organic semiconductors used. The electrode pick-up stripes are labelled with (1) and (2) (PEDOT: PSS), and (3) and (4) (Al). Indicated by dots and arrows is the measurement sequence. b) Cross section of the device. c) Scheme of the signal readout. d) Measured signal ratio. e) Signal ratio values projected onto the *x*,*y*-plane.

x- and log (I_3/I_4) to the *y*-coordinate as defined in Figure 1a. The excitation intensity only influences the absolute currents, not the signal ratio. This also means that the device works under illumination from both sides or, if illuminated through a filtering layer, without any modifications of the readout or data processing. The maximum and minimum signal ratios of a channel define a signal range that depends on the sheet resistance of the respective electrodes. In this example, an *x*-range of $0.086\,\mathrm{cm}^{-1}$ and a *y*-range of $0.031\,\mathrm{cm}^{-1}$ can be derived with $350\,\Omega\ \square$ and $200\,\Omega\ \square$ in the respective electrodes. This range implies that with these electrode sheet resistances, significantly larger elements can reach a high level of sensitivity. Details on this are posted online as Supplementary Information.

In Figure 1e, the signal ratios are projected onto the *x*,*y*-plane and compared with the real positions of the light spot on the sample. To achieve a good correlation, an offset correction has to be applied to shift the coordinates (*x*: +0.2365; *y*: +0.126) and a scaling factor to convert the signal ratio into centimetre values (*x*: × 11.65; *y*: × 38.1). The resulting mean deviation is about 3 mm (*x*: 1.2 mm; *y*: 2.3 mm).

In Figure 2, the possibilities of tuning the position detection are discussed. A second device was built on a PEDOT:PSS-covered PET foil with a sheet resistance of 1.5 kΩ □. The sheet resistance of the Al top electrode is measured to be approx. 140 Ω □. A scan over the surface of this sample results in the characteristics shown in Figure 2a. The signal range in the *y*-direction (correlated with the Al electrode) is smaller ($0.018\,\mathrm{cm}^{-1}$) than that of the previous sample (*x*: 350 Ω □; *y*: 200 Ω □), while the range in the *x*-direction is more than doubled to $0.18\,\mathrm{cm}^{-1}$. This shows the direct correlation between the sheet resistances of the electrodes and the signal range in the corresponding direction. From the present measurements, the dependence of the signal range on the size and electrode resistance can be roughly given as $1.5 \times 10^{-4}\,\mathrm{cm}^{-1}(\Omega\ \square)^{-1}$.

To achieve an offset to the signal ratio, the simple addition of a resistor in the outer circuit of a channel suffices. This is shown in Figure 2b, where 300 Ω is added to channel 2, shifting the signal ratio of the *x*-direction up by 0.25 while leaving the signal ratio in the *y*-direction unchanged. Although this allows a simple tuning of the device performance, it also means that external resistances owing to cable lengths, contacting, etc. have to be controlled and compensated.

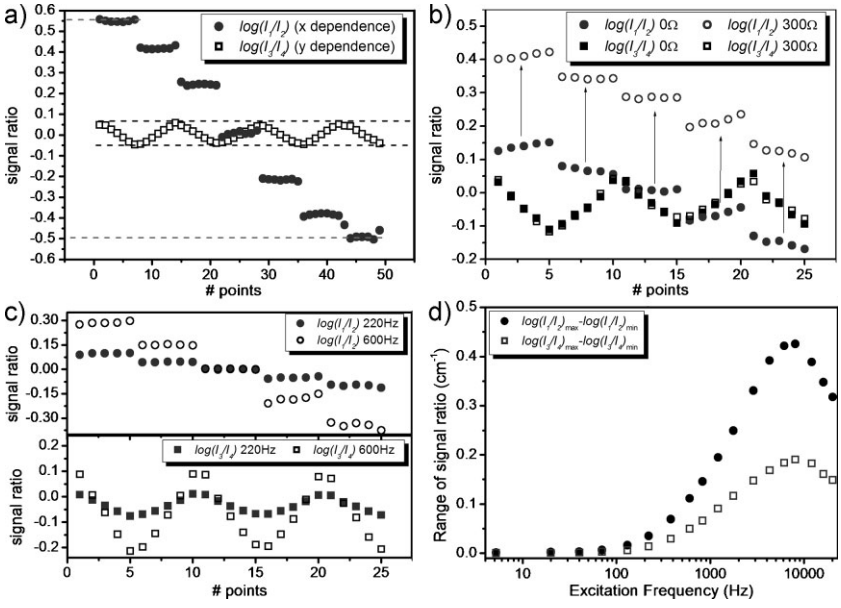

Figure 2. Tunability of the position sensitive device. a) Measured signal ratio for a device with a PEDOT: PSS sheet resistance of 1.5 kΩ/□. b) Measured signal ratio before and after adding 300 Ω to channel 2. c) Measured signal ratio for two different excitation frequencies. d) Range of signal ratios depending on different excitation frequencies.

The interplay of capacitances and resistances along and through the device has a strong influence on the temporal dependencies of the current signal. Therefore, the performance of the device is tunable by changing the modulation frequency of the excitation light. This is shown in Figure 2c, where the values of the signal ratio are more than doubled after changing the frequency from 220 to 600 Hz.

The dependence of the range of signal ratio on excitation frequency is plotted in Figure 2d, where a strong correlation can be observed. At low frequencies, the device behaves as if the sheet resistance of the electrodes increases strongly with the frequency: it reaches a maximum at about 8 kHz and then decreases again. Thus, the sensitivity of the PSD is tuned over a large range by changing the excitation frequency. This facilitates the production of devices with enormously different sizes, as the same electrodes can be used and the signal range tuned to fit the readout electronics by changing the frequency of excitation. A mathematical model is under development to analyze the temporal behaviour of the device as a two-dimensional distributed network of capacitors and resistances, whch results in a diffusive transport of the photogenerated charge carriers to the output channels.

To further illustrate the usefulness of this concept, a simple addition to the device has been designed to achieve touchpad functionality. On the PSD, a 4 mm thick waveguide fabricated from the transparent elastomer polydimethylsiloxane (PDMS) is placed. Outside the active area of the position detector, 16 red LEDs modulated with 170 Hz are mounted so that part of their light is coupled into planar waveguide modes of the PDMS. As the PDMS waveguide is transparent, the device retains its full light-point sensing capability without any modification to the data readout and processing.

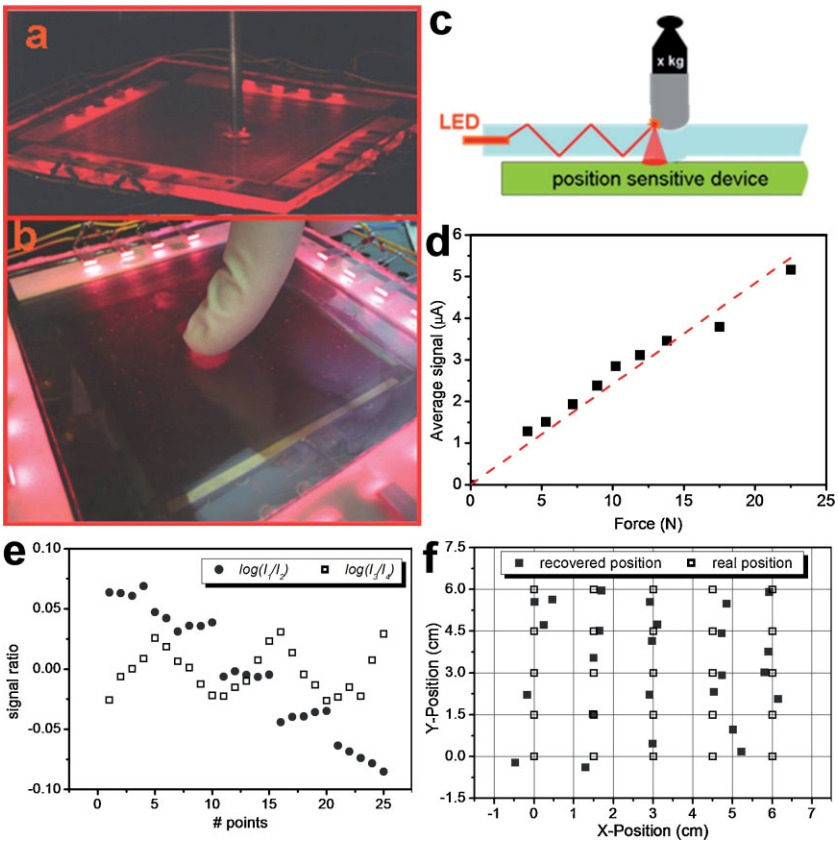

Figure 3. Adding touchpad functionality to the position sensitive device. a) Photograph of the touchpad device with a metal bar coupling light out of the PDMS waveguide. b) Photograph of the touchpad device with a finger coupling light out of the waveguide. c) Scheme of the touchpad with the large area photodiode and an elastomer touchpad. d) Photocurrent versus force applied to the metal bar. e) Signal ratio scanning the surface of the touchpad with a metal bar. f) Projection of the signal ratio on the *x*,*y*-plane.

Putting localized pressure on the PDMS sheet deforms it and light is scattered out of the waveguide mode onto the PSD, which can detect the site where the pressure is applied. The working principle is sketched in Figure 3c. Figure 3a shows the measurement setup with a metal bar of 6 mm diameter and a rounded tip, which is pushed with various forces onto the PDMS waveguide. In Figure 3b the touchpad device can be seen under operation with a finger.

Figure 3d shows the average current signals of all channels with different pressures applied on the metal bar. In the range up to 20 N, the currents rise approximately linearly with a slope of ~250 nA N^{-1}, making the device a quantitative detector for localized pressure. This means that the device can sense the pressure exerted on its surface, which could be used to encode further functions to touchpoints such as the thickness of a digital line drawn with a finger or stylus.

As fingers have a larger surface area with stronger scattering than the metal bar, the current signal coming from the finger applying a very small pressure is already more than 10 μA. In addition, the pressure sensitivity could be further tuned by using PDMS with different crosslink densities and, therefore, varying stiffness.[11]

To ascertain the functionality of the extended device as a position sensitive touchpad, the metal bar is pressed with approx. 15 N on the surface in a 6 × 6 cm^2 raster with 15 mm distance between the measurement points. As the diodes cannot be reliably operated at high frequencies, the range of signal ratios is small. However, a clear dependence on the position is observable in Figure 3e. The projection onto the *x*,*y*-coordinates shown in Figure 3f gives a mean error of about 5.5 mm (*x*: 1.9 mm; *y*: 4.8 mm). Likely reasons for this error are inaccuracies in the positioning and the low signal to noise ratio because of the low excitation frequency.

As the light is scattered out of the waveguide in a non-uniform fashion onto a rather large spot on the surface of the detector, a precise positioning is not possible. But for following a finger

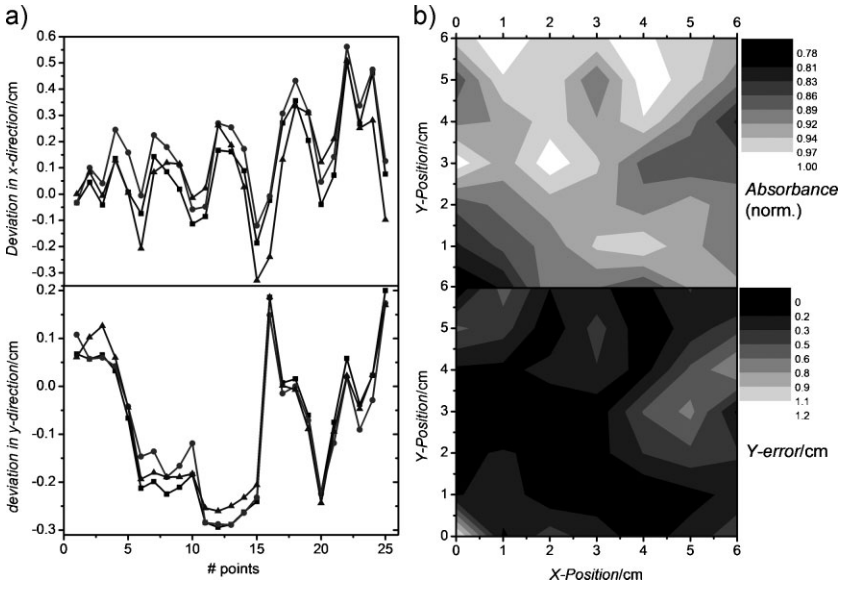

Figure 4. Investigating the source of signal deviations. a) Deviation of the recalculated position in the *x*- (upper panel) and *y*-direction (lower panel) in three consecutive measurement runs, showing the high reproducibility of the recalculated positions and, therefore, the possibility to achieve a much better precision by calibrating the device. Upper panel: Absorbance of the device at 780 nm measured in a raster across the surface, visualizing the inhomogeneous distribution in the thickness of the aluminum electrode. Lower panel: Deviation of signal projection from real light point position in the *y*-direction, which reveals a correlation of signal deviation and thickness non-uniformity of the metal back electrode.

touchpoint over a large surface in the square meter range, the accuracy of the detector seems already sufficient.

Recalculating the position with the simple algorithm used here assumes a homogeneous sheet resistance of the electrodes. Although inhomogeneities in the charge generation layer of the photodiode do not influence the results, inhomogeneities or misalignment in the electrodes will give rise to deviations of the recalculated position values. To obtain extremely precise position information, the device fabrication has to be optimized or deviations have to be calibrated for each device. The calibration route is especially interesting since it allows keeping the production efforts low.

In Figure 4a, the deviations between the recovered and real position in the *x*- (lower panel) and *y*-direction (upper panel) are plotted for three consecutive measurements in a 5×5 point raster. The difference in the recovered position values between consecutive scans is far below 1 mm in most points. Thus, a calibrated device can achieve a precision of better than 1 mm on a single photodetector with an area of 49 cm^2 with only four contacts. A matrix device would need 4900 photodetector pixels and corresponding signal lines to achieve the same resolution for lightpoint detection.

The most important reason for deviations of the calculated from the real *x*,*y*-position of the light point has been identified in the inhomogeneity of the metal electrode. Because of the geometrical setup of the available evaporation chamber, as well as the strain applied during the hot-lamination process, the thin aluminum electrode has different thicknesses and, therefore, conductivities in different places. These inhomogeneities especially affect the recalculation of the *y*-position. By measuring the absorbance of the device at 780 nm, a wavelength where the active layer absorption is negligible compared with the extinction of the aluminum electrode; inhomogeneities in the thickness of the metal layer are visualized.

In the upper panel of Figure 4b, the absorbance of different spots of the device is shown in a contour plot that can be compared with the contour plot of the deviation of the projected signal in the *y*-direction from the real position as shown in the lower panel. A correlation between the two graphs is revealed. In places with low absorbance, where the metal electrode is thinner or damaged, the corresponding recalculated *y*-values show a higher deviation from the real *y*-position of the light spot. There is no correlation with the deviation in the *x*-direction, which is generally significantly smaller.

This is not the only source of error in the position recalculation where the uniformity of the electrode sheet resistance is assumed, but gives an indication as to which changes may lead to further improvements of this new class of position sensitive devices. However, by means of calibration such inaccuracies can be taken into account and devices with minor faults and deviations can yield precise position sensing. In addition, refined models of signal generation that take into account local variations in sheet resistances may be used for recalculation.

In summary, a large area, semitransparent and flexible device capable of determining the magnitude and absolute position of light- and touch-points has been fabricated. A product family based on this technology platform can present a new approach towards multifunctional human interface devices added onto or below a screen, thus ridding the computers of today of the large number of cumbersome display and input devices. In addition, the possibility to detect the position and the pressure of a touch signal in a flexible device makes this technology interesting as a sensor foil for the artificial skin of robots and other machinery.

Experimental

Device Fabrication: The devices were fabricated on 8 cm × 8 cm substrates of PET foils coated with PEDOT: PSS obtained from AGFA-Gevaert. To avoid contact problems and shorts, the PEDOT: PSS coating was removed by scratching with a wet cotton tip from about 4 mm distance of two opposing edges of the substrate to result in a strip of PEDOT:PSS 8 cm long and 7 cm wide spanning the substrate. Approx. 4 mm wide and 7 cm long strips of 100 nm thick Ag were deposited by thermal evaporation along the other two edges to give a good contact to the PEDOT: PSS electrode.

Afterwards, a layer of 50 nm C_{60} blended 1: 1 by volume with ZnPc followed by 30 nm of pure C_{60} was thermally evaporated under high vacuum ($P < 10$–5 mbar, 1 mbar = 100 Pa) onto the whole substrate. The diode was formed with the evaporation of a strip of Al 7 cm wide and 8 cm long perpendicular to the PEDOT:PSS electrode. To achieve a homo-

geneous pickup from the Al electrode, two strips of 100 nm thick Al 4 mm wide and 7 cm long were added on the edges where the PEDOT: PSS was removed.

The whole device was then run through a standard office hot laminator with a 150 μm thick PET foil on each side to protect it against environmental stress. Cables were glued to the pickup lines with conducting silver paste through little holes in the lamination foils. After a slight initial decrease of the current output, the performance stayed stable over weeks with the device stored and measured under standard office and laboratory conditions.

The touchpad extension was fabricated using the PDMS base and hardener system Sylgard with a mixing ratio of base to hardener of 20:1. A first layer with ~1 mm thickness and 15 cm × 15 cm area was spread on a glass plate and hardened at about 50 °C in an oven. The LEDs were then placed onto the first layer with four LEDs at each edge of the layer. The extension was finished by spreading and hardening another layer of 3 mm thickness over the LEDs and the first layer, to yield a PDMS sheet of 4 mm thickness with four red LEDs embedded at each side.

The position sensitive device was fixed under the PDMS waveguide by a 1 mm thick double-sided adhesive tape that also acted as a spaceholder to prevent out-coupling of light from the waveguide without pressure applied.

Measurement Setup: The position sensitive device was measured using a 10 mW, 532 nm green laser diode module that illuminated the sample through an OD1 filter, thus yielding an optical intensity of 0.8 mW on the sample, which is typical for the output power of a standard laserpointer for purposes of presentation. To filter out any background signal, the illumination was chopped with a mechanical chopper at different frequencies and the currents were measured with a lock-in amplifier after a current to voltage converter. To scan the surface of the sample, it was mounted on an *x*,*y*-translation stage and moved under the light beam. The repositioning error of the stage is less than 0.1 mm.

The touchpad was measured by using a metal bar with 6 mm diameter, which was loaded with different weights to push the bar onto the surface of the PDMS waveguide. To measure the position sensitivity, the sample was fixed on the translation stage and moved under the metal bar. An electronic scale was used to quantify the force applied on the metal bar by the weights. As some of the light was coupled from the PDMS waveguide into the position sensitive device without the metal bar being pressed onto the device, a background signal was determined before applying the pressure and subtracted from the measurement signal.

To estimate the homogeneity of the aluminum back electrode, the absorbance as –log (transmission) was measured at different locations by measuring the light power of a 5 mW 780 nm laser after passing the beam through the sample. As baseline, the average absorbance of an unfinished sample without the metal back electrode was taken. The diameter of the laser beam transmitted through the device was about 2.5 mm.

Acknowledgements

The authors thank Franz Bürscher for his suggestions, Lisa Fallon for technical assistance, and Louis Bollens from AGFA-Gevaert for providing the ORGACON foils. Work was partially supported by the Austrian Science Funds (FWF) within the National Research Network on Functional Organic Films. Supporting Information is available online at Wiley InterScience or from the author.

Received: February 17, 2009
Revised: May 8, 2009
Published online: July 6, 2009

[1] N. S. Sariciftci, D. Braun, A. J. Heeger, *Appl. Phys. Lett.* **1993**, *62*, 585.
[2] C. W. Tang, *Appl. Phys. Lett.* **1986**, *48*, 183.
[3] P. Peumans, A. Yakimov, S. R. Forrest, *J. Appl. Phys.* **2003**, *93*, 3693.
[4] T. Someya, Y. Kato, S. Iba, Y. Noguchi, T. Sekitani, H. Kawaguchi, T. Sakurai, *IEEE Trans. Electron Dev.* **2005**, *52*, 2502.
[5] J. Henry, J. Livingstone, *Adv. Mater.* **2001**, *13*, 1023.
[6] D. Kabra, Th, B. Singh, K. S. Narayan, *Appl. Phys. Lett.* **2004**, *85*, 5073.
[7] B. P. Rand, J. Xue, M. Lange, S. R. Forrest, *IEEE Photon. Technol. Lett.* **2003**, *15*, 1279.
[8] G. Buchberger, R. Schwoediauer, S. Bauer, *Appl. Phys. Lett.* **2008**, *92*, 123511.
[9] T. Someya, T. Sekitani, S. Iba, Y. Kato, H. Kawaguchi, T. Sakurai, *Proc. Natl. Acad. Sci. USA* **2004**, *101*, 9966.
[10] R. Koeppe, N. S. Sariciftci, A. Büchtemann, *Appl. Phys. Lett.* **2007**, *90*, 181126.
[11] G. Bar, L. Delineau, A. Häfele, M.-H. Whangbo, *Polymer* **2001**, *42*, 3527.